Modeling Effect of Fragment Impact Orientation and Shape on Explosive Response[1]

Ryan Conner* and Jon Conner

CS Squared LLC, 21448 N. 75th Ave., Ste. 12, Glendale, AZ 85308 USA

Email: ryan.conner@cssquared.onmicrosoft.com

Abstract

The Fragment Impact Test, as described in STANAG 4496 [1], is conducted to assess the violence of reaction of a munition subjected to high-velocity impact of a fragment meant to simulate an aerial bomb or artillery projectile fragment. The standard fragment used to simulate aerial bomb or artillery fragments, as described in Annex A of STANAG 4496 [1], is designed to facilitate gun launch of the fragment while inducing minimal pitch or yaw. Due to the asymmetry of the fragment design and the requirement to conduct only a single test for a given impact location, however, future tests may include costly efforts to measure the orientation of the fragment at impact, where this measurement is not currently required by the testing standard. This leaves the question, what is effect of fragment impact orientation on the response of a munitions' high explosive fill, and is this effect significant enough to potentially invalidate a test? This paper was prepared to present results of a computational study performed to examine the effects of small fragment impact angle deviations from 0°, specifically 2°, 5°, 10°, and 20° on the initial transient pressure response in a notional munition filled with Composition B high explosive when subjected to the standard (8300 ft/s) fragment impact test as described in STANAG 4496 (Edition 1). This paper also presents, for comparison, results of models performed using a spherically shaped steel fragment of the same mass.

I. Introduction

To simulate the effects of fragment orientation on the initial transient pressure in the high explosive fill just beneath the shell casing wall following impact, three continuum mechanics finite element models were developed. The simplified models are meant to simulate a notional 155 mm diameter munition with varying steel casing thicknesses filled with Composition B. The 155 mm shell thicknesses modeled and described herein are 0.5", 0.25", and 0.125", respectively. Composition B was selected as the explosive fill for this study as it is a common melt pour explosive fill for mortar and artillery projectiles and a calibrated reactive flow model has been published for it. All three models were run with the fragment impacting at five different orientations; 0°, 2°, 5°, 10°, and 20°, with 0° being the fragment oriented with its cylindrical axis perpendicular to the munition shell body axis of symmetry as intended in the test.

In addition, this paper presents the results of a computational study performed to compare the initial transient pressure response due to a spherical fragment of the same mass and material as the standard conical fragment currently used for test. These results are compared to the results of the standard fragment at 0° to determine if the spherical fragment is a feasible replacement for the standard fragment. Switching from a conical fragment to a spherical fragment would remove

[1] This work was funded by Booz Allen Hamilton Prime Contract Number FA8075-14-D-0016, Task DS 17-1531. The views, opinions and findings, contained in this report are those of the author(s) and should not be construed as an official Department of Defense (DOD) position, policy, or decision, unless so designated by other official documentation.

the need for measuring fragment orientation at impact, as the spherical fragment would be completely symmetrical.

All the finite element models presented in this report were meshed using the commercial software program Trelis, developed and marketed by Computational Simulation Software, LLC (csimsoft). They were run using the commercial software program, LS-DYNA, developed and marketed by Livermore Software Technology Corporation (LSTC). The test description and material parameters used to run these models were obtained from the open literature and unclassified, publicly released, distribution unlimited, sources.

II. Fragment Impact Test: General Setup

A three-dimensional (3D), half-symmetry, explicit Lagrangian finite element model was built to simulate the fragment impact test. A notional 155 mm diameter munition was modeled with a 2:1 length to diameter aspect ratio. Figure 1 shows the 3D half-symmetry model with a 0.5" shell thickness of 4340 steel and the standard fragment of mild steel oriented at an impact angle of 0°. The remaining two models had a similar configuration with the same outer diameter of 155 mm and aspect ratios, the main difference being the reductions in shell thickness resulted in more high explosive mass to fill the gap left by the thinner shell. In all cases reported here the fragment impact velocity modeled was 8300 ft/s (2350 m/s).

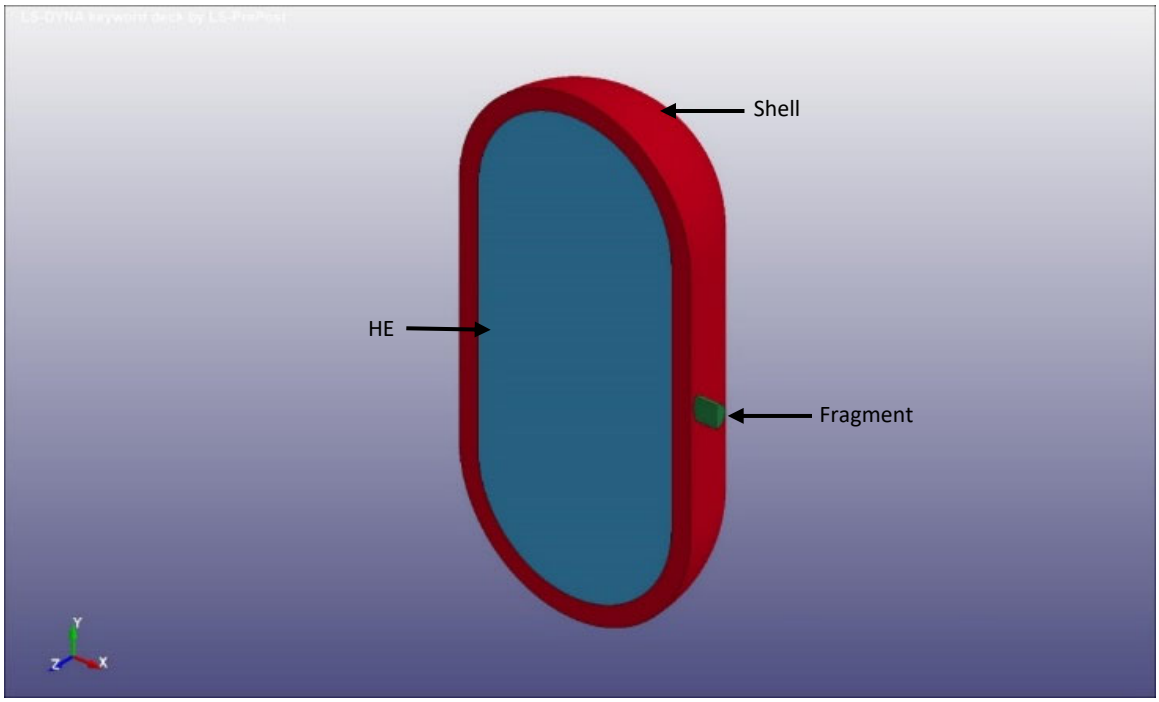

Figure1. 3D Half-Symmetry Model of Fragment Impact Test.

The high explosive material was modeled using a reactive flow ignition and growth model for Composition B, a mixture of TNT and RDX. To implement this model an unreacted constitutive model was required for the high explosive sample. The constitutive model selected was an Elastic/Plastic Hydrodynamic material model, with the parameters used taken from reference [2]. To model the shock to detonation properties of the Composition B high explosive material the

Ignition and Growth reactive flow model was implemented as the equation of state, with parameters taken from reference [3].

The steel munition casing and the standard steel fragment plastic deformation, damage accumulation, and material failure were modeled using a Johnson-Cook constitutive material model with the parameters taken from references [4-7]. Both material equations of state were modeled using the Mie-Gruneisen equation of state with the parameters taken from references [8] and [9].

The interface between the steel munition casing and the steel fragment was modeled using the eroding sliding contact algorithm in LS-DYNA to enable material failure of the elements while retaining the mass of the failed material at the interface as nodes. The finite element mesh was created using Trelis. All three had a mesh resolution of approximately 20 zones/cm.

III. Results – Standard Fragment

The simulation was run with the fragment in five different orientations at impact: 0°, 2°, 5°, 10°, and 20°. Each simulation was run for a total of 8 μsec with single precision (32 bit) accuracy using the LS-DYNA solver “ls-dyna_smp_s_Dev_125010_winx65.exe”. In all cases the fragment initial velocity was 8300 ft/s (2530 cm/ μsec), corresponding to the standard test in reference [1]. To illustrate the model geometry with a fragment off axis, Figure 2 provides a general view of the model before impact with the fragment oriented at 10°, and a shell casing thickness of 0.5”. To demonstrate the typical results observed in all of simulations run, Figure 3 presents a pressure contour of this model at 2, 4, 6, and 8 μsec after fragment impact. This illustrates the shock to detonation occurring in the Composition B high explosive material predicted by the model at the 10° fragment impact orientation. All other orientations exhibited a similar shock to detonation behavior in the Composition B explosive fill.

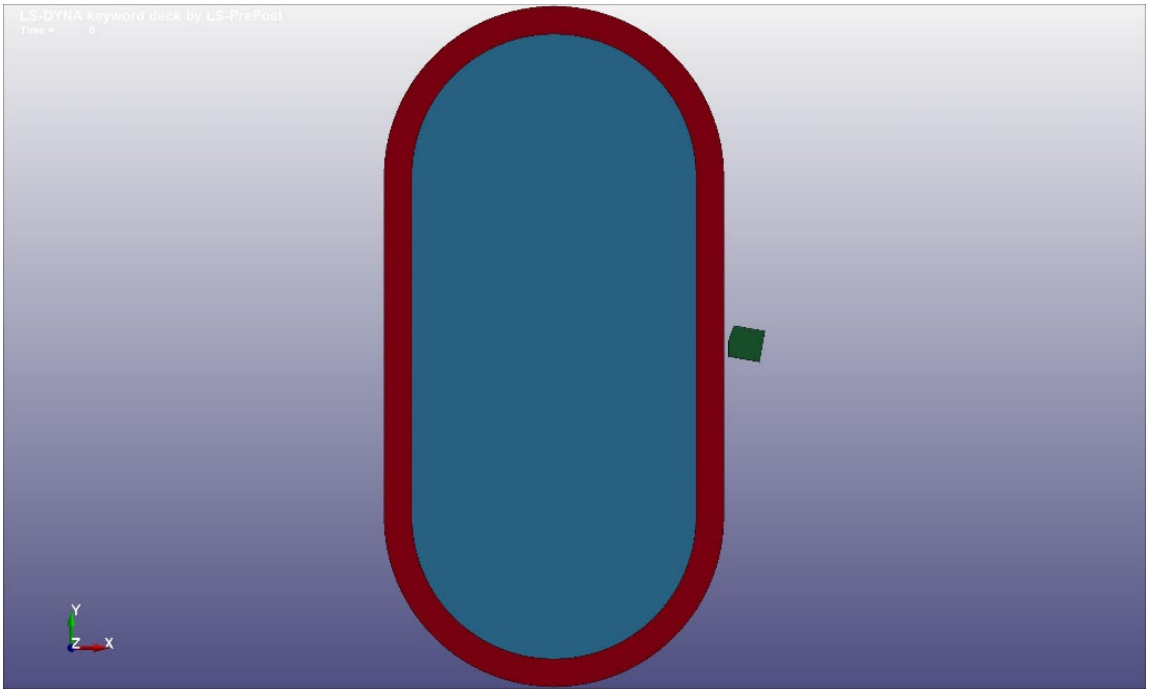

Figure 2. General View - 10° Fragment Impacting 0.5” Thick Shell Casing.

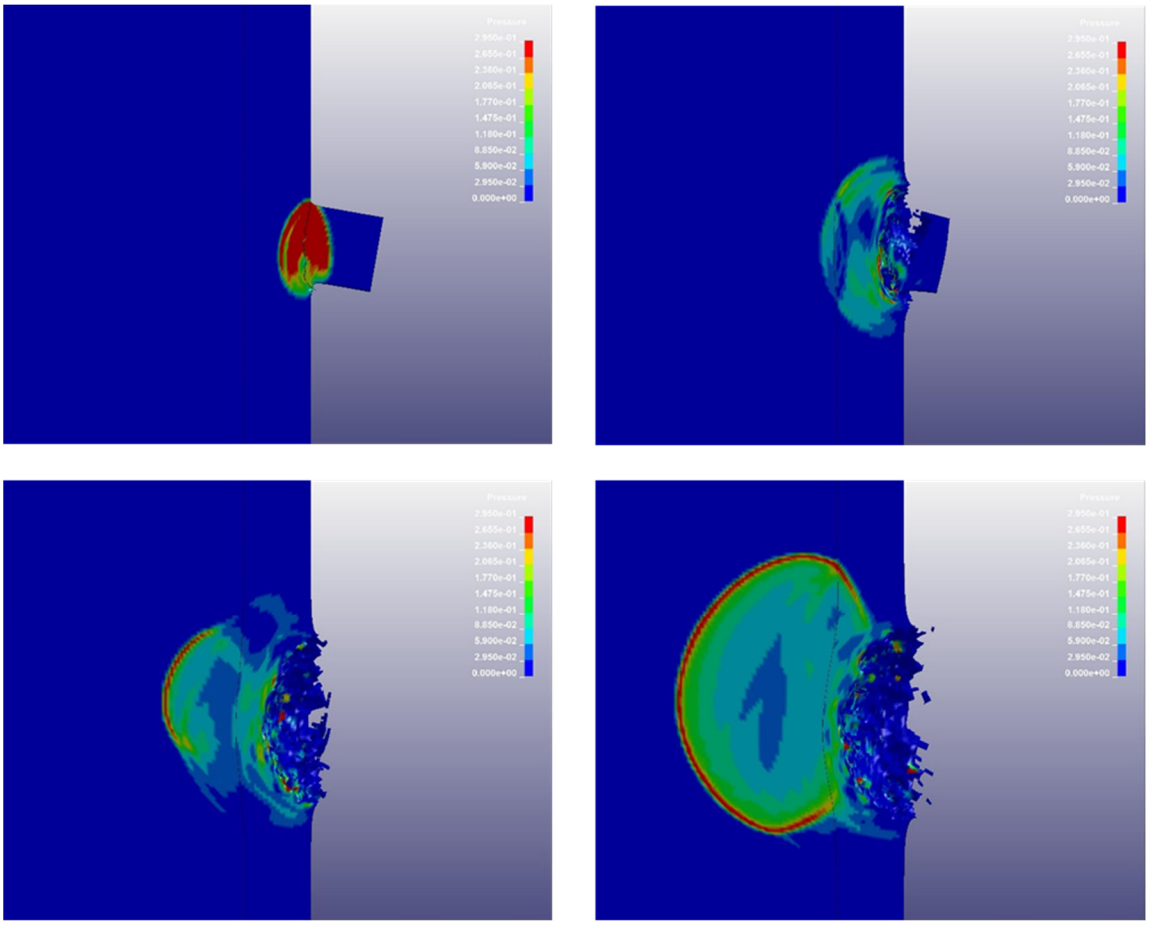

Figure 3. 10° Fragment – Pressure Contours at 2, 4, 6, and 8 μs After Impact.

For each simulation, a pressure-time history was recorded for one element in the Composition B high explosive material closest to the explosive/shell casing interface that experienced the highest initial pressure after fragment impact. The predicted pressure was recorded for this element every 0.001 µsec. Figure 4 presents a pressure vs. time history comparison for the elements selected at the five different fragment impact orientations for a 0.5” shell casing thickness.

Table 1 presents a summary of the peak pressure experienced in the high explosive immediately after impact for each shell casing thickness (0.5”, 0.25”, and 0.125”) at the five different fragment orientations (0°,2°,5°,10°, and 20°).

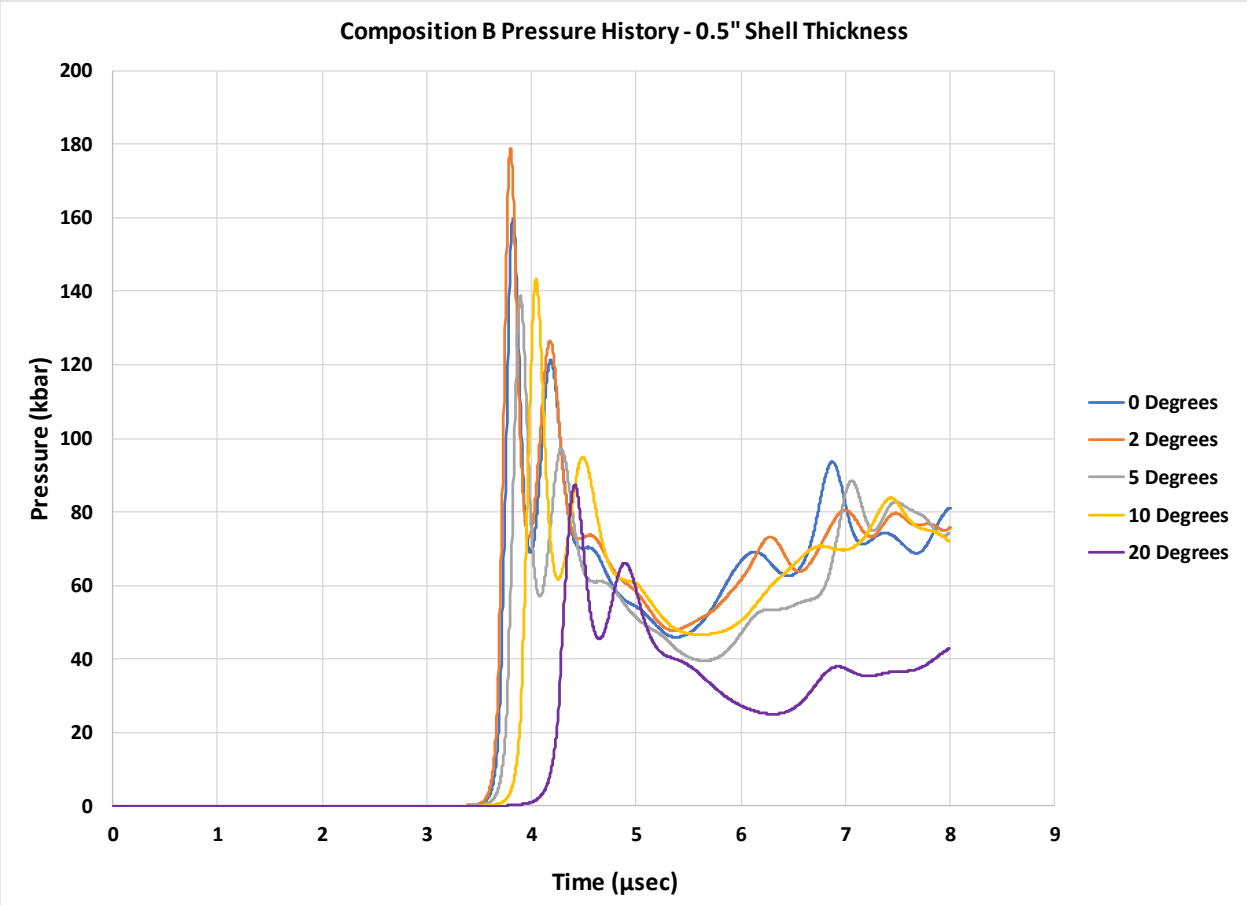

Figure 4. Composition B Pressure vs. Time History for 0.5” Shell Casing Thickness

Table 1. Peak Pressure Summary of Results for Standard Fragment.

0.5” Shell Casing Peak Pressure Summary		
Fragment Orientation (°)	Peak Pressure (kbar)	Percent Change from 0°
0	160	
2	179	12%
5	139	-13%
10	143	-10%
20	88	-45%
0.25” Shell Casing Peak Pressure Summary		
Fragment Orientation (°)	Peak Pressure (kbar)	Percent Change from 0°
0	249	
2	272	9%
5	274	10%
10	291	17%
20	286	15%
0.125” Shell Casing Peak Pressure Summary		
Fragment Orientation (°)	Peak Pressure (kbar)	Percent Change from 0°
0	310	
2	346	12%
5	297	-4%
10	294	-5%
20	295	-5%

For a shell casing thickness of 0.5”, the initial peak shock pressure experienced in the high explosive material sees a maximum with a fragment orientation of 2°, with an orientation of 5°, 10° resulting in a slight decrease (maximum of 13%) when compared to 0°, and 20° resulting in a larger 45% decrease.

For a shell casing thickness of 0.25”, it was observed that the initial peak shock pressure experienced in the high explosive material increases slightly at all fragment orientations modeled when compared to 0°. Impact orientations of 10° and 20° produced the highest peak pressures and were near the Chapman-Jougout pressure for Composition B of 295 kbar, resulting in immediate detonation.

For a shell casing thickness of 0.125”, the initial peak shock pressure experienced in the high explosive at all orientations were near or exceeded the Chapman-Jouguet pressure of 295 kbar, resulting in immediate detonation.

IV. Fragment Impact Test: Spherical Fragment General Setup

To eliminate the need for measuring fragment impact angle upon impact, one possible solution is to replace the current conical fragment with a fully symmetrical spherical fragment. To investigate this solution, the same 3D, half-symmetry, explicit Lagrangian finite element models of varying shell thicknesses presented previously were utilized, with the conical fragment replaced with a spherical fragment of the same mass. All materials and material properties remained as previously described. In all cases the fragment impact velocity modeled was 8300 ft/s (2350 m/s).

Figure 5 illustrates the 3D half-symmetry model with a 0.5” shell thickness of 4340 steel and a spherical fragment of mild steel.

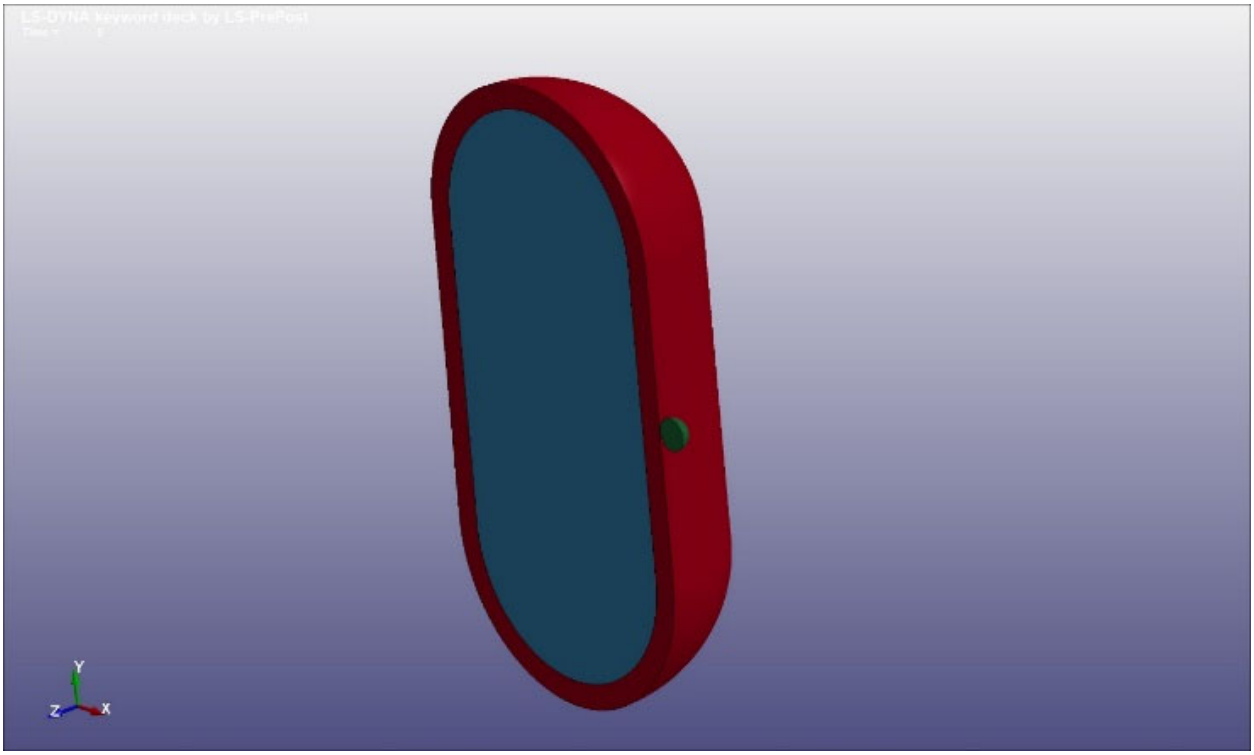

Figure 5. 3D Half-Symmetry Model of Spherical Fragment Impact Test.

V. Results – Spherical Fragment

Each spherical fragment simulation was run for a total of 8 μsec with single precision (32 bit) accuracy using the LS-DYNA solver “ls-dyna_smp_s_Dev_125010_winx65.exe”. Figure 6 provides a general view of the model before impact, with a shell thickness of 0.25”. To illustrate the typical results observed in all simulations, Figure 7 shows pressure contours for the model at 2, 4, 6 and 8 μsec after fragment impact with a 0.25” shell thickness. This illustrates the shock to detonation occurring in the Composition B high explosive material predicted by the model at all shell thicknesses.

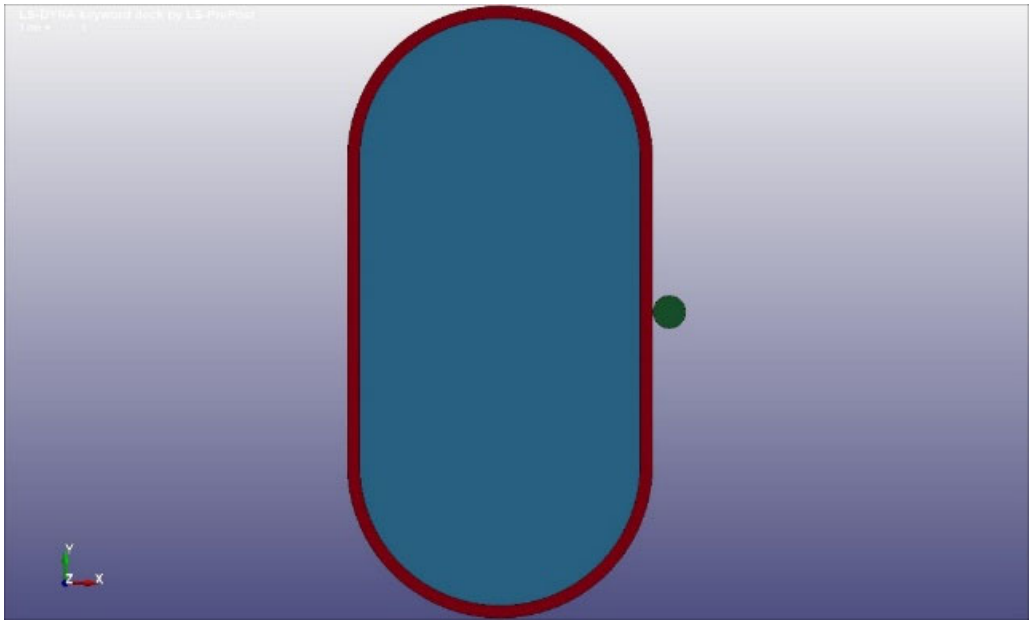

Figure 6. General View – Spherical Fragment Impacting 0.25” Shell Casing.

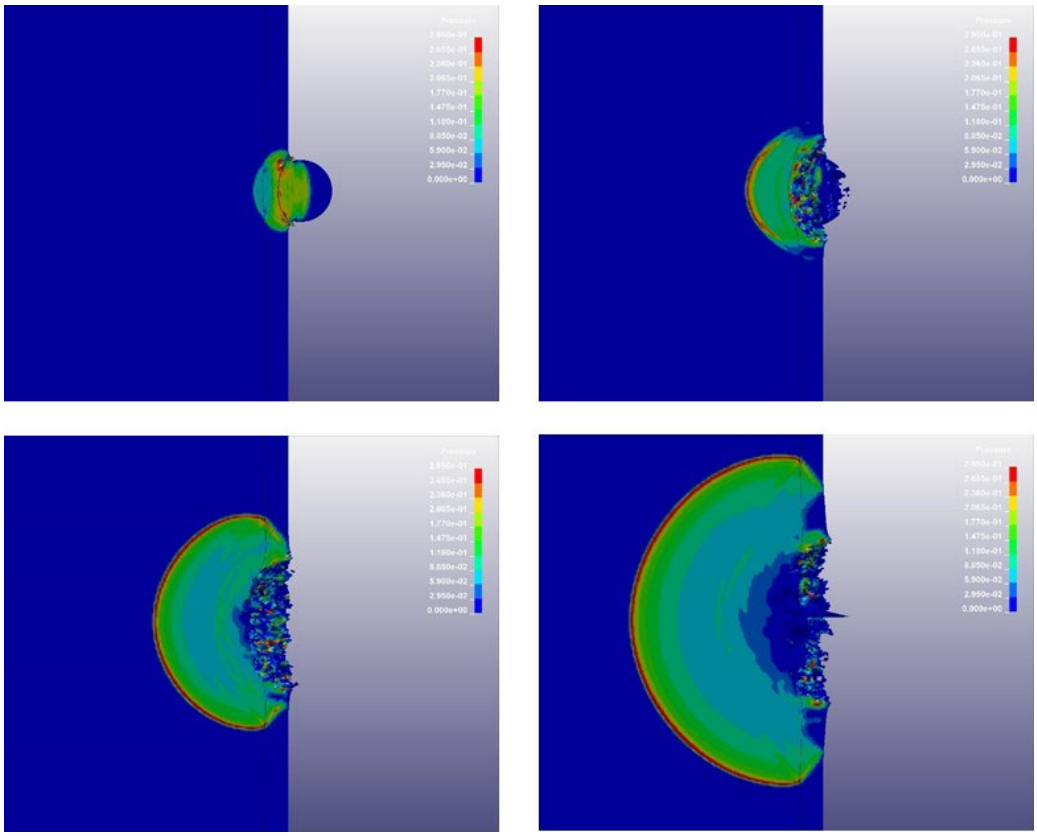

Figure 7. Spherical Fragment – Pressure Contours at 2, 4, 6, and 8 µs After Impact.

As was recorded for the conical fragment, a pressure-time history was recorded for one element in the high explosive material closest to the high explosive/shell interface that experienced the highest initial pressure after fragment impact. The predicted pressure was recorded for the

element every 0.001 µsec. Figure 8 provides a pressure vs. time history comparing high explosive elements from the spherical and conical fragment simulations for a shell thickness of 0.25". Results for all simulations with varying shell thicknesses are summarized in Table 2.

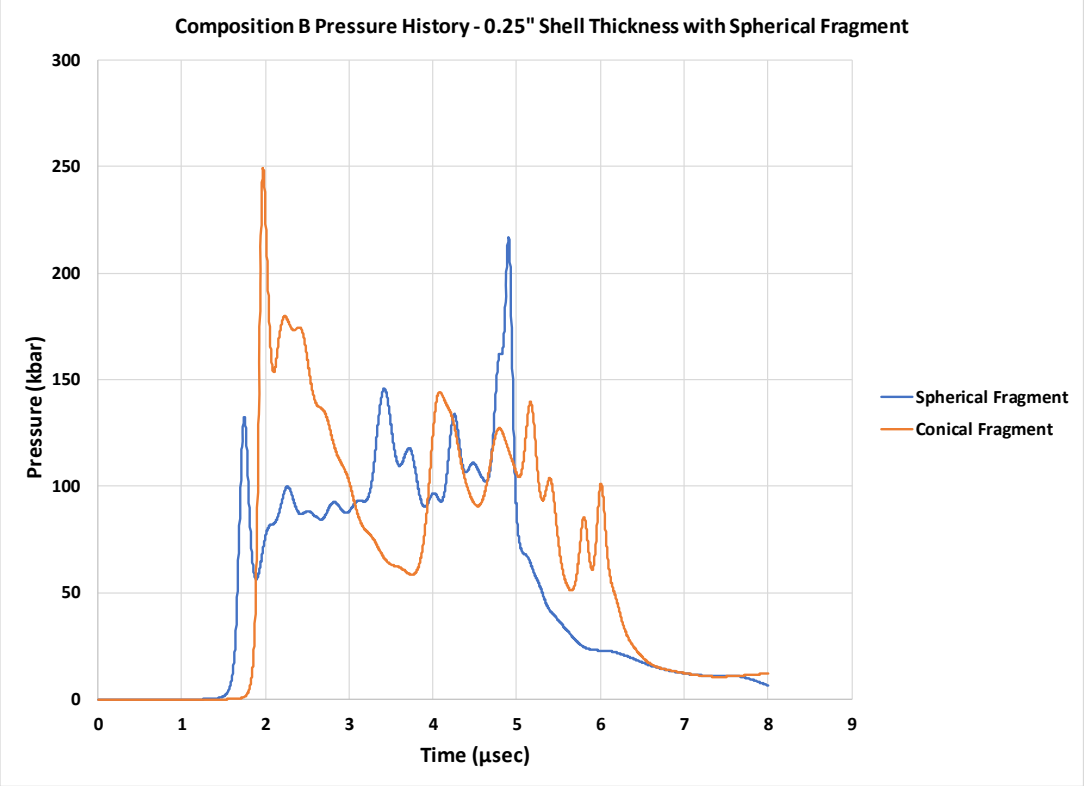

Figure 8: Composition B Pressure vs. Time History for 0.25" Shell Casing Thickness.

Table 2. Peak Pressure Summary of Results for Spherical Fragment.

0.5" Shell Casing Peak Pressure Summary		
Fragment Type	Peak Pressure (kbar)	Percent Change from 0°
Conical	160	
Spherical	59	-63%
0.25" Shell Casing Peak Pressure Summary		
Fragment Type	Peak Pressure (kbar)	Percent Change from 0°
Conical	249	
Spherical	132	-47%
0.125" Shell Casing Peak Pressure Summary		
Fragment Type	Peak Pressure (kbar)	Percent Change from 0°
Conical	310	
Spherical	249	-20%

Notably the initial peak shock pressure experienced in the high explosive due to a spherical fragment is significantly lower than that due to the conical fragment with all shell thicknesses.

VI. Summary and Conclusions

The fragment impact test [1] is conducted to simulate the effects of a high velocity impact due to an aerial bomb or artillery fragment on a munition and to measure the violence of the response. Due to the asymmetry of the standard fragment design used to simulate a bomb/artillery shell, concerns have been raised as to the effect of the orientation of the fragment upon impact with the munition under test. To address this concern, the modeling reported here examined minor deviations from the intended impact orientation of 0° that would be plausible in an actual gun fired test; specifically, 2°, 5°, 10°, and 20°. Also explored was the replacement of the standard conical fragment with a symmetrical spherical fragment, which would alleviate asymmetry concerns completely.

Results of the conical fragment simulations show that minor deviations in fragment orientation and its effect on the shock pressure time history experienced in the explosive fill can vary based on shell thickness. For a 0.5” thick shell, a 2° deviation resulted in a slight increase (12%) in peak pressure relative to 0°, while orientations of 5° and 10° resulted in slight decreases in peak pressure (13% and 10% respectively). 20° resulted in a more significant drop of 45%. With a 0.25” and 0.125” shell thickness, all deviations from 0° resulted in a slight increase in peak pressures. With a 0.25” shell, fragment orientations of 10° and 20° resulted in the immediate detonation of Composition B. With a 0.125” shell, all orientations simulated resulted in immediate detonation.

Results of the spherical fragment simulations showed significant drops in the peak pressure experienced in the explosive fill at all shell thicknesses modeled, which unfortunately indicates a spherical fragment that is of the same mass and material as the current conical fragment is likely not an acceptable replacement for the current fragment design.

References

1. NATO Standardization Agreement (STANAG) 4496, Edition 1, Fragment Impact, Munitions Test Procedure, 13 December 2006.
2. Dobratz, B.M., LLNL Explosives Handbook, Properties of Chemical Explosives and Explosive Simulants, UCRL-52997, DE85-015961, University of California, Livermore, CA, 1981.
3. Urtiew, P.A., Vandersall, K.S., Tarver, C.M., Garcia, F., Forbes, J.W., Shock Initiation of Composition B and C-4 Explosives: Experiments and Modeling. Russian Journal of Physical Chemistry B, Vol. 2, No. 2, pp. 162-171, ISSN 1990-7931, 2008.
4. Banerjee, B., The Mechanical Threshold Stress Model for Various Tempers of AISI 4340 Steel. Vol. 44, Issues 3-4, pp. 834-859, ISSN 0020-7683, 2007.
5. MMPDS-07: Metallic Materials Properties Development and Standardization (MMPDS). Federal Aviation Administration, 2012.
6. Johnson, G.R. and Cook, W.H., A Constitutive Model and Data for Metals Subjected to Large Strains, High Strain Rates, and High Temperatures. Proceedings 7th International Symposium on Ballistics, The Hague, pp. 541-547, 19-21 April 1983.
7. Johnson, G.R. and Cook, W.H., Fracture Characteristics of Three Metals Subjected to Various Strains, Strain Rates, Temperatures and Pressures. Engineering Fracture Mechanics, Vo. 21, No. 1, pp. 31-48, ISSN 0013-7944, 1985.
8. Kohn, B.J., Compilation of Hugoniot Equations of State. Air Force Weapons Laboratory Report No. AFWL-TR-69-38, Kirtland Air Force Base, NM, 1969.
9. Iqbal, M.A., Senthil, K., Bhargava, P., Gupta, N.K., The Characterization and Ballistic Evaluation of Mild Steel. International Journal of Impact Engineering, Vol. 78, pp. 98-113, ISSN 0734-743X, 2015.